Protective structures with waiting links and their damage evolution *

Andrej Cherkaev   Liya Zhornitskaya [†]

September 9, 2003

Abstract

The paper is concerned with simulation of the damage spread in protective structures with "waiting links." These highly nonlinear structures switch their elastic properties whenever the elongation of a link exceeds a critical value; they are stable against dynamic impacts due to their morphology. Waiting link structures are able to spread "partial damage" through a large region, thereby dissipating the energy of the impact. We simulate various structures with waiting links and compare their characteristics with conventional designs. The Figures show the damage propagation in several two-dimensional structures.

Keywords: Dynamics of damage. Failure. Structures.
AMS classification: 70K75, 37N15, 74D10

1 Introduction. Waiting elements and spread of damage

This paper describes protective structures that exhibit an unusually high dissipation if they are subject to a concentrated (ballistic) impact. Under this impact, the structure experiences a very large forces applied during a short time. The kinetic energy of the projectile must be absorbed in the structure. We want to find a structure that absorbs maximal kinetic energy of the projectile without rupture or breakage. Here, we consider dilute structures. Specifically, we define the structure as an assembly (network) of rods connected in knots. The structure may be submerged into a viscous substance.

While theoretically a material can absorb energy until it melts, real structures are destroyed by a tiny fraction of this energy due to material instabilities and an uneven distribution of the stresses throughout the structure. Therefore, we increase the stability of the process of damage by special morphology of the structural elements.

1

The increase of the stability is achieved due to special structural elements used for the assembly: the so-called "waiting links". These elements contain parts that are initially inactive and start to resist only when the strain is large enough; they lead to large but stable pseudo-plastic strains; structures distribute the strain over a large area, in contrast to unstructured solid materials where the strain is concentrated near the zone of an impact. Similar structures are considered in [1], [4], [6], [9], [10]. The continuum models are discussed in [2]; experimental study is performed in [8].

In this paper we introduce a model for dynamic failure of links made from brittle-elastic materials, discuss the dynamics of networks of waiting links, a model of the penetrating projectile and the criteria of resistance of deteriorating structure. We simulate the damage spread in the lattices and optimize their parameters. The figures demonstrate elastic waves and waves of damage in the lattices and visualize the damage evolution.

2 Equations and algorithms

2.1 Brittle-elastic bar

Consider a stretched rod from a homogeneous elastic-brittle material. If slowly loaded, this material behaves as a linear elastic one, unless the length z reaches a critical value z_f, and fails (becomes damaged) after this. The critical value z_f is proportional to the length L of the rod at equilibrium

$$z_f = L(1 + \epsilon_f) \tag{1}$$

where the critical strain ϵ_f is a material's property. The static force F_{static} in such a rod depends on its length z as

$$F_{static}(z) = \begin{cases} ks(z/L - 1) & \text{if } z < z_f \\ 0 & \text{if } z \geq z_f \end{cases} \tag{2}$$

where k is an elastic modulus and s is the cross-section of the rod.

Dynamic model of damage increase We are interested to model the dynamics of damageable rods; therefore we need to expand the model of brittle material adding the assumption of the dynamics of the failure. We assume that the force F in such a rod depends on its length z and on the *damage parameter* c:

$$F(z, c) = ks(1 - c)(z/L - 1) \tag{3}$$

where K is the elastic modulus. The damage parameter c is equal to zero if the rod is not damaged and is equal to one if the rod is destroyed; in the last case the force obviously is zero. Development of the damage is described as the increase of the damage parameter $c(z, t)$ from zero to one. The damage parameter equals zero in the beginning of the deformation and it remains zero until a moment

when the elongation exceed the critical value; it can only increase in time. This parameter depends on the history of the deformation of the sample.

We suggest to describe the increase of damage parameter by the differential equation

$$\frac{d\,c(z,t)}{d\,t} = \begin{cases} v_d & \text{if} \quad z \geq z_f \text{ and } c < 1 \\ 0 & \text{otherwise} \end{cases} \quad , \quad c(0) = 0 \qquad (4)$$

where z_f is the maximal elongation that the element can sustain without being damaged, and v_d is the speed of damage. This equation states that the damage increases in the instances when the elongation exceeds the limit z_f; the increase of damage stops if the element is already completely damaged. The speed v_d can be chosen as large as needed.

Remark 1 *The damage can also be modeled by a discontinuous function c_H that is equal to zero if the element is undamaged and to one if it is damaged:*

$$c_H(z,t) = \lim_{v_d \to \infty} c(z,t).$$

Consideration of continuously varying damage parameter (4) instead of a discontinuous one increases stability of the computational scheme.

Remark 2 *One can argue about the behavior of the rod with an intermediate value of the damage parameter. We do not think that these states need a special justification: they simply express the fact that the stiffness rapidly deteriorates to zero when the sample is over-strained. We notice that in the simulations presented here the time of transition from undamaged to damaged state is short.*

2.2 Waiting links

Here we introduce special structural elements – waiting links – that several times increase the resistivity of the structure due to their morphology. These elements and their quasistatic behavior are described in [1]. The link is an assembly of two elastic-brittle rods, lengths L and Δ ($\Delta > L$) joined by their ends (see Figure 1, left). The longer bar is initially slightly curved to fit. When the link is stretched by a slowly increasing external elongation, only the shortest rod resists in the beginning. If the elongation exceeds a critical value, this rod breaks at some place between two knots. The next (longer) rod then assumes the load replacing the broken one.

Assume that a unit amount of material is used for both rods. This amount is divided between the shorter and longer rod: the amount α is used for the shorter (first) rod and the amount $1 - \alpha$ is used for the longer (second) one. The cross-sections s_1 and s_2 of rods are:

$$s_1(\alpha) = \frac{\alpha}{L} \quad \text{and} \quad s_2(\alpha) = \frac{1-\alpha}{\Delta}, \qquad (5)$$
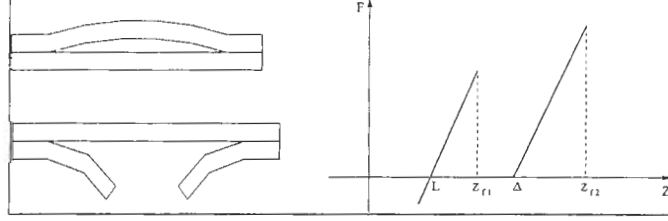
Figure 1: Left above: The waiting link in the initial state. Left below: The waiting link after the first rod is broken. Right: The force-versus-length dependence for a monotone elongation

The force-versus-elongation dependence in the shorter rod is:

$$F_1(z) = k s_1(\alpha) \left(\frac{z}{L} - 1\right)(1 - c_1) \qquad (6)$$

where $c_1 = c_1(z,t)$ is the damage parameter for this rod; it satisfies the equation similar to (4)

$$\frac{d c_1(z,t)}{dt} = \begin{cases} v_d & \text{if } z \geq z_{f_1} \text{ and } c_1(z,t) < 1 \\ 0 & \text{otherwise} \end{cases} \qquad c_1(z,0) = 0 \qquad (7)$$

where $z_{f_1} = L(1 + \epsilon_f)$.

The longer rod starts to resist when the elongation z is large enough to straighten this rod. After the rod is straight, the force-versus-elongation dependence is similar to that for the shorter rod:

$$F_2(z) = \begin{cases} k s_2(\alpha) \left(\frac{z}{\Delta} - 1\right)(1 - c_2), & \text{if } z \geq \Delta \\ 0, & \text{if } z < \Delta \end{cases} \qquad (8)$$

Here F_2 is the resistance force and $c_2 = c_2(z,t)$ is the damage parameter for the second rod:

$$\frac{d c_2(z,t)}{dt} = \begin{cases} v_d & \text{if } z \geq z_{f_2} \text{ and } c_2(z,t) < 1 \\ 0 & \text{otherwise} \end{cases} \qquad c_2(z,0) = 0 \qquad (9)$$

These equations are similar to (6), (7), where the cross-section $s_1(\alpha)$ is replaced by $s_2(\alpha)$ and the critical elongation z_{f_1} by $z_{f_2} = \Delta(1 + \epsilon_f)$. The difference between the two rods is that the longer (slack) rod starts to resist only when the elongation is large enough.

The total resistance force $F(z)$ in the waiting link is the sum of $F_1(z)$ and $F_2(z)$:

$$F(z) = F_1(z) + F_2(z). \qquad (10)$$

The graph of this force-versus-elongation dependence for the monotone external elongation is shown on Figure 1 (right) where the damage parameters jump from zero to one at the critical point z_{f_1}.

One observes that the constitutive relation $F(z)$ is nonmonotone. Therefore one should expect that the dynamics of an assembly of such elements is characterized by abrupt motions and waves (similar systems but without damage parameter were investigated in [5, 6]).

2.3 Dynamics

It is assumed that the inertial masses m_i are concentrated in the knots joined by the inertialess waiting links (nonlinear springs), therefore the dynamics of the structure is described by ordinary differential equations of motion of the knots. We assume that the links are elastic-brittle, as it is described above. Additionally, we assume that the space between the knots is filled with a viscous substance with the dissipation coefficient γ. The role of the viscous media is important: We will demonstrate that even a slow external excitation leads to intensive waves in the system, the energy of this waves are eventually adsorbed by the viscosity. Without the viscosity, the system never reaches a steady state.

The motion of ith knot satisfies the equation

$$m_i \ddot{\mathbf{z}}_\mathbf{i} + \gamma \dot{\mathbf{z}}_\mathbf{i} = \sum_{j \in N(i)} \frac{F_{ij}(|\mathbf{z}_\mathbf{i} - \mathbf{z}_\mathbf{j}|)}{|\mathbf{z}_\mathbf{i} - \mathbf{z}_\mathbf{j}|} (\mathbf{z}_\mathbf{i} - \mathbf{z}_\mathbf{j}) \qquad (11)$$

where $\mathbf{z}_\mathbf{i}$ is the vector of coordinates of ith knot, $|.|$ is length of the vector, $N(i)$ is the set of knots neighboring the knot i, m_i is the mass of the ith knot. The force F_{ij} in the ijth link depends on the damage parameters $c_{ij,1}$ and $c_{ij,2}$ as in (10). The set of neighboring knots depends on geometric configuration.

Remark 3 *In this model, the masses are permitted to travel as far as the elastic links permit. Particularly, when these links are completely broken, the concentrated mass moves "between" other masses without interaction with them.*

Below in Section 4.4, we discuss a special model for the projectile that is "large enough" and does not slip through the rows of linked masses.

Setting The speed of waves in a structure is of the order of the speed of sound in the material which the structure is made of (approximately 5,000 m/sec for steel). In our numerical experiments, we assume that the speed of the impact is much smaller (recall that the speed of sound in the air is 336 m/sec). A slow-moving projectile does not excite intensive waves in stable structures, but it does excite mighty waves of damage in the waiting structure. The reason is that the energy stored in the elastic links suddenly releases when the links are broken. This phenomenon explains the superb resistance of the waiting structure: The energy of the projectile is spent to excite the waves of damage.

2.4 Numerical algorithm

To solve the system (11) numerically, we first rewrite it as an autonomous system of first order differential equations:

$$\dot{\mathbf{z}}_\mathbf{i} = \mathbf{p}_\mathbf{i}, \qquad (12)$$

$$\dot{\mathbf{p_i}} \;\; = \;\; \frac{1}{m_i}(\phi_i - \gamma\mathbf{p_i}), \tag{13}$$

where

$$\phi_i = \sum_{j\in N(i)} \frac{F_{ij}(|\mathbf{z_i} - \mathbf{z_j}|)}{|\mathbf{z_i} - \mathbf{z_j}|}(\mathbf{z_i} - \mathbf{z_j}). \tag{14}$$

Introducing the notation

$$\vec{\mathbf{x}} = \{\mathbf{z_i}, \mathbf{p_i}\}\,, \quad \vec{\mathbf{f}} = \left\{\mathbf{p_i}, \frac{1}{m_i}(\phi_i - \gamma\mathbf{p_i})\right\},$$

we get

$$\dot{\vec{\mathbf{x}}} = \vec{\mathbf{f}}(\vec{\mathbf{x}}).$$

We solve the resulting system via the second order Runge-Kutta method

$$\vec{\mathbf{x}}_{n+1} = \vec{\mathbf{x}}_n + \frac{k}{2}\left(\vec{\mathbf{f}}(\vec{\mathbf{x}}_n) + \vec{\mathbf{f}}(\vec{\mathbf{x}}_n + k\vec{\mathbf{f}}(\vec{\mathbf{x}}_n))\right), \tag{15}$$

where k denotes the time step. Note that the stability condition of the resulting method depends on the damage speed v_d from (7),(9) and the dissipation coefficient γ. In all numerical experiments that follow we establish convergence empirically via time step refinement.

3 Damage of a homogeneous strip

We consider a homogeneous strip made as a triangular lattice with waiting links. The left side of the strip is fixed while the right one is pulled with a given constant speed V.

The three next figures show the comparison of damage evolution in the waiting link structures (Figures 2, 3, $\alpha = 0.25$) and the structure from conventional brittle-elastic materials (Figure 4; $\alpha = 1.0$). Intact waiting links (both rods are undamaged) are shown by bold lines; partially damaged links (the shorter rod is destroyed, the longer one is undamaged) correspond to dashed lines; destroyed links (both links are damaged) are not shown.

Figures 2 and 3 illustrate an interesting phenomenon: controllability of the wave of damage. If the speed V is high, the wave of "partial breakage" (colored blue) propagates starting from the point of impact; when the wave reaches the other end of the chain, it reflects and the magnitude of stress increases; at this point, the chain breaks. Notice that the breakage occurs in the opposite to the impact end of the chain. If the speed is smaller, the linear elastic wave propagates instead of the wave of partial damage; the propagation starts at the point of impact. When the wave reaches the opposite end of the strip and reflects, it causes the wave of partial damage that propagated toward the point of impact. Later, the strip breaks near the point of impact (not shown).

Figures 3 and 4 compare the waiting link structures to conventional brittle-elastic structures (with the same pulling speed V and final time). One can see
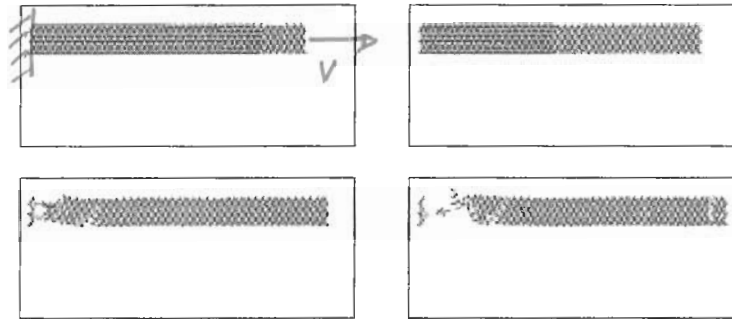
Figure 2: Evolution of damage in a fastly pulled lattice with waiting elements (α=25%).
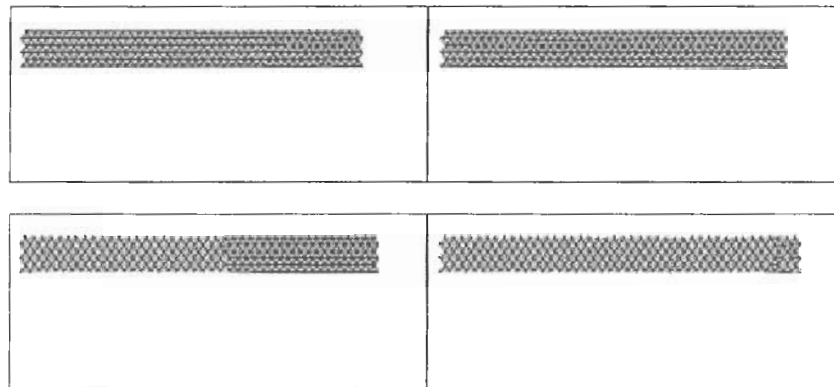

Figure 3: Evolution of damage in a slowly pulled lattice with waiting elements (25%).
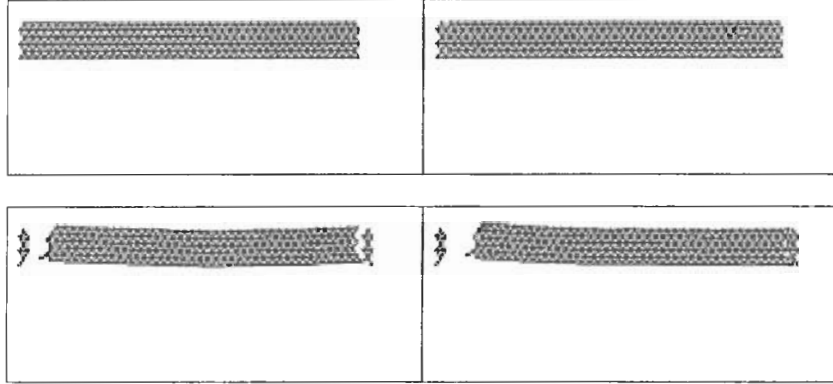
Figure 4: Evolution of damage in a slowly pulled lattice without waiting elements (α=1).

that the conventional strip breaks near the point of impact as well as near the fixed side. Note that only several links in the conventional structure break while all others stay undamaged. To the contrary, the waiting link structure spreads "partial damage" through the whole region, thereby dissipating the energy of the impact. As a result, the waiting link strip preserves the structural integrity due to absorbing the kinetic energy of the pulling.

Remark 4 *The direct comparison of conventional and waiting link structures is not easy: the energy dissipated in a conventional structure is proportional to its crossection (Figure 4) while the energy dissipated in the waiting link structure is proportional to its volume (Figure 3).*

4 Structures under a concentrated impact

In this section, we investigate the resistance and failure of structures from waiting links impacted by a massive concentrated projectile. The kinetic energy of the projectile must be absorbed in the structure without its total failure.

4.1 Model of the projectile

Modeling the projectile, one needs to take into account the penetration of it through the structure, and prevent it from slipping through the line of knots. Therefore one cannot model the projectile as another "heavy knot" in the structure with an initial kinetic energy: Such model leads to the failure of the immediate neighbor links after which the projectile slips through the net without interaction with other knots.

In our experiments, the projectile is modeled as an "elastic ball" of the mass M_p centered at the position z_p. Motion of the mass satisfies the equation

$$M_p \ddot{\mathbf{z}}_{\mathbf{p}} = \sum_j \frac{F_{pj}(|\mathbf{z}_{\mathbf{p}} - \mathbf{z}_{\mathbf{j}}|)}{|\mathbf{z}_{\mathbf{p}} - \mathbf{z}_{\mathbf{j}}|} (\mathbf{z}_{\mathbf{p}} - \mathbf{z}_{\mathbf{j}}) \qquad (16)$$

similar to (11), but the force F_{pj} is found from the equation

$$F_{pj}(z) = \begin{cases} 0 & \text{if} \quad z > B \\ \ln\left(\frac{B-A}{z-A}\right) & \text{if} \quad A < z \leq B \\ +\infty & \text{if} \quad z \leq A \end{cases} \qquad (17)$$

In the numerical experiments that follow $A = 0.5L$, $B = 2L$.

This model states that a repulsive force is applied to the knots when the distance between them and $\mathbf{z}_{\mathbf{p}}$ is smaller than a threshold B. This force grows when the distance decreases and become infinite when the distance is smaller than A. This model roughly corresponds to the projectile in the form of a nonlinearly elastic ball with a rigid nucleus. When it slips through the structure, the masses in the knots are repulsed from its path causing deformation and breaks of the links.

4.2   Effectiveness of a design

Comparing the history of damage of several designs, we need to work out a quantitative criterion of the effectiveness of the structure. This task is nontrivial, since different designs are differently damaged after the collision.

Effectiveness criterion   We suggest an integral criterion that is not sensitive to the details of the damage; instead, we are measuring the variation of the impulse of the projectile. It is assumed here that the projectile hits the structure flying into it vertically down.

To evaluate the effectiveness, we compute the ratio R in the vertical component $p_v = \mathbf{p}_P \cdot (0,1)$ of the impulse $\mathbf{p}_P$ of the projectile before and after the impact:

$$R = \frac{p_v(T_{final})}{|p_v(T_0)|} \qquad (18)$$

where T_0 and T_{final} are the initial and the final moments of the observation, respectively. The variation of impulse of the projectile R shows how much of it is transformed to the motion of structural elements. Parameter R evaluates the structure's performance using the projectile as the measuring device without considering the energy dissipated in each element of the structure; it does not varied when the projectile is not in a contact with the structure.

Different values of the effectiveness parameter are presented in the Table 1. An absolute elastic impact corresponds to the final impulse opposite to the initial one; therefore in this case $R = -1$. The absence of the structure correspond to

Effect	Range of R
Elastic contact with a rigid plane	-1
Projectile is rejected	(-1, 0)
Plastic contact (the projectile stops)	0
Projectile breaks through	(0, 1)
No effect	1

Table 1: Effectiveness parameter R

$R = 1$, because the impulse of the projectile does not change. If the projectile stops then $d = 0$; if it breaks through the structure; then $R \in (0, 1]$; and if it is rejected, then $R \in [-1, 0)$. The smaller R is, the more effective the structure is.

Other criteria   Other criteria compare the state of the structure before and after the collision. These criteria are applicable only if the structure (or its pieces) after the collision reach a steady state. This is why we need the dissipation factor in the model. Without this factor, the elastic waves never stop and their interference caused additional damage to the structure any time after the collision.

We register several criteria:

1. The percentage of partially damaged links.

2. The percentage of destroyed links.

The first number shows how effective the damage is spread, and the second shows badly the structure is damaged. Ideally, we wish to have a structure in which all elements are partially damaged, but no element is completely destroyed.

Remark 5 *The number of destroyed element is a rough quality criterion. It ignores a significant factor - the positions of the destroyed links.*

4.3   Bridge-like designs

Next figures (Figures 5 and 6) show the dynamics of the damage of a bridge-like truss structure made from waiting links (1). The structure is supported by its vertical sides. The horizontal sides are free. It is impacted by a projectile that is modeled as an "elastic ball" (4.1). The projectile impact the center of the upper side of the structure moving vertically down with an initial speed v_0. If the speed is small, the projectile is rejected, otherwise it penetrates through the structure. The difference in the impulse of the projectile before and after the impact shows the effectiveness of the structure. The number of destroyed links also represent the effectiveness showing how much the damage is spread. Dynamic constitutive relation for each element is described as a damageable link 2.3.
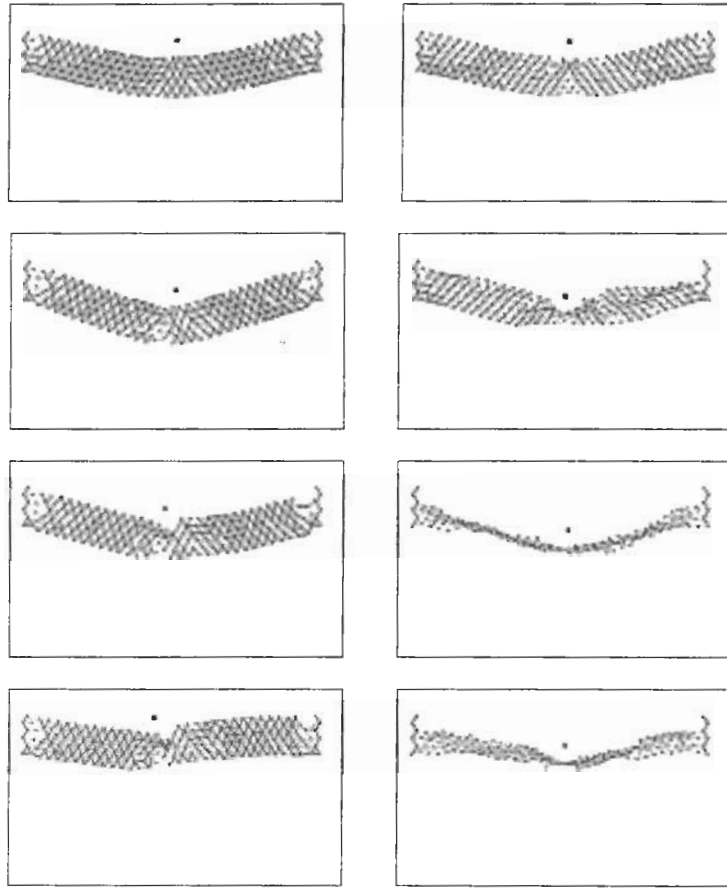
Figure 5: Evolution of damage in a lattice with waiting elements (left column α=25%, right column: α=10%).
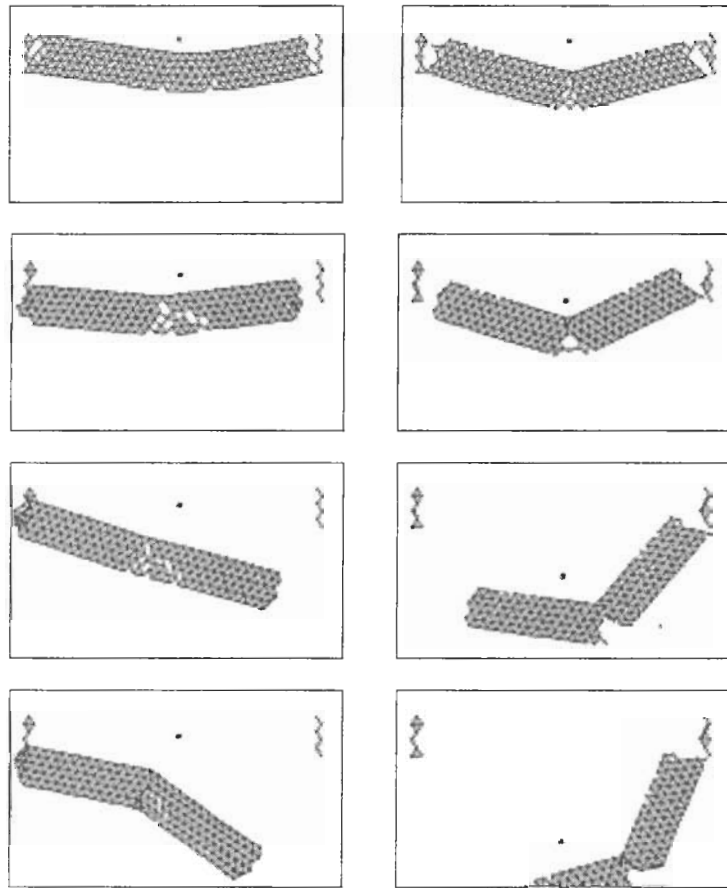
Figure 6: Evolution of damage in a lattice with (right, α=50%) and without (left α=25%)) waiting elements.

Figure	α	% of damaged links	% of destroyed links	Effective-ness R	Final time T_{final}
Fig. 5 (right)	0.10	94%	3.8%	-0.26	500
Fig. 5 (left)	0.25	42%	3.8%	-0.32	500
Fig. 6 (right)	0.50	4.6%	6.3%	0.54	250
Fig. 6 (left)	1.00	0%	8.6%	0.46	250

Table 2: Damage and/or destruction of a bridge.

We simulate the damage process of the bridge by varying the parameter α (the fraction of material put into the shorter link) while keeping the other parameters ($L, \Delta, z_{f_1}, z_{f_2}$, total amount of material, etc.) the same for all runs. The results of the simulation are summarized in Table 2. One can see from Table 2 that as α decreases from 1.00 (conventional structure) to 0.10 the percentage of partially damaged links increases as the percentage of destroyed links decreases making the structure more resistant. Table 2 also shows that $\alpha = 0.25$ is optimal for both minimizing the number of destroyed links and minimizing the effectiveness parameter R (see the discussion in Section 4.2).

Figures 5 and 6 show the damage evolution of the impacted structures that differ by the value of α. Intact waiting elements (both links are undamaged) are shown by bold lines; partially damaged elements (the short link is destroyed, the longer one is undamaged) correspond to dotted lines; destroyed elements (both links are damaged) are not shown. The snapshots are taken at equal time intervals. The final time of simulation for Figure 5 (unbroken construction) is twice smaller than for Figure 6 (broken construction).

See chapter 3

The structures with $\alpha = .50$ and $\alpha = 1.00$ (conventional structure) soon develop cracks and fall apart allowing the projectile to go through (see Figure 6) while the structures with $\alpha = 0.10$ and $\alpha = 0.25$ preserve the *structural integrity* by dissipating energy and taking the stress away from the point of impact; this results in the rejection of the projectile (see Figure 5). Notice that the final time T_{final} is twice as small in the last two examples.

The propagation of the damage is due to several factors: the local instabilities of the part of the network that contains a damaged link: the force acting on neighboring links significantly increases and the damage spreads; the waves that propagate through the network and initiate the damage in the remote from the collision point areas.

4.4 Damage of a massive structure

This section describes the result of simulation of damage/destruction of network made from the waiting links and compares these structures with the nets from conventional links.

This series of experiments aims to show the wave of damage and strains in a "large" domain (the block). The block is supported from the sides, the bottom is free (see Figure 7). As in the above mentioned simulations of the bridges, the block is impacted by a projectile that is modeled as an "elastic ball" (Section 4.1). It is assumed that the projectile hits the center of the upper side of the structure moving vertically down with an initial speed v_0.

Figure 7 demonstrates propagation of the elastic waves and the waves of partial and total damage of elements of the block. Conventional link structure soon develops cracks and gets destroyed while the waiting link structure preserves its structural integrity. Notice that the damage is concentrated in conventional design and spread in the waiting link design.

5 Discussion

Resume

1. Our numerical experiments have demonstrated the possibility of control of the damage process: Waiting links make it is possible to increase the resistivity, increase the time of rupture, increase the absorbed energy, and decrease the level of concentration of damage.

2. The results emphasize the necessity of dynamics simulation versus computation of the quasi-static equilibrium: one can see (Figure 7) that damage can start in parts of the structure distant from the zone of impact. Development of damage is caused by excited waves and local instabilities.

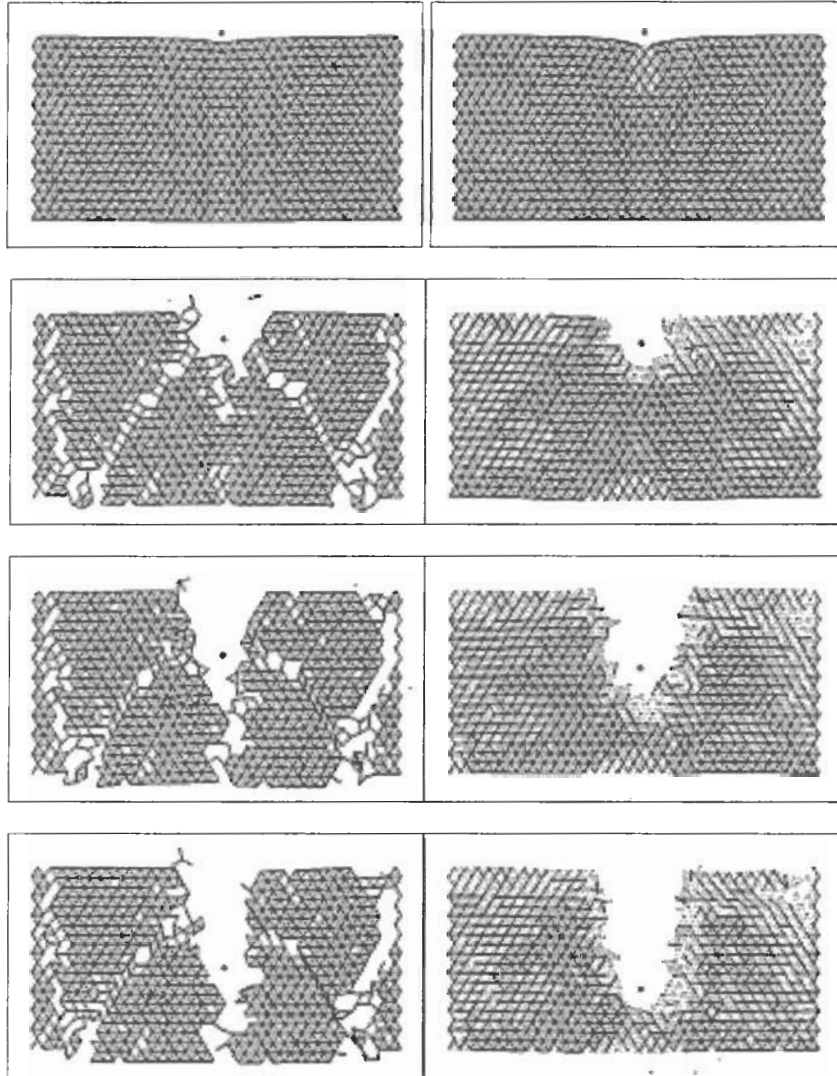3. We observe that the results strongly depend on parameters of the structure and projectile.

Figure 7: Evolution of damage in a lattice with waiting elements. Left field: lattice from elastic-brittle material; right field: lattice from waiting links, $\alpha=.25$

Continuum and discrete model

We use a discrete model of the construction rather then the continuous equation for several reasons. First, it models the structures that can be made as we described. However, one may ask how simplify the computation of the dynamics using a homogenized description of the networks. The process of damage is similar to the process of phase transition, since the initial (undamaged) phase is replaced by the partially damaged state and then by the destroyed state of structure in a small scale; these processes can be described as a phase transition in solids, see for example [3].

However, the observed process is also significantly controlled by intensive waves caused by vibration of individual masses. The fast-oscillating motion carries significant energy and it is responsible for initiation of the damage in the parts of the structure that are not connected to the zone of impact, but are close to reflecting boundaries. In the continuum model, these oscillation would become infinite fast and the corresponding waves would propagate with infinite speed. It is still unclear how to describe these effects in the homogenized model.

Optimization

The demonstrated structures show the ability to significantly increase the resistance comparing with conventional materials. However, this results are still far away from the limit that can be achieved by optimizing the response by new design variables: The ratio α and the additional (slack) length $(\Delta - L)$ of the waiting rod. In principle, these parameters can be separately assigned for each link, keeping the total amount of material fixed. However, there are natural requirement of robustness: A structure should equally well resist all projectiles independently of the point of impact, and should well resist projectiles approaching with various speed. This consideration decreases the number of controls; it is naturally to assign the same values of the design parameters for all elements in the same level of the structure.

One may minimize the absorbed energy, restricting the weight, admissible elongation, and the threshold after which the damage starts. In addition, one needs to restrict the range of parameters of a projectile: Its mass, direction, and speed. The range of parameters is important: Because of strong nonlinearity, the qualitative results are expected to be sensitive to them. The optimization problem is computationally very intensive since the dependence of parameters is not necessary smooth or even continuous. We plan to address the optimization problem in the future research.

References

[1] A. Cherkaev, and L. Slepyan. Waiting Element Structures and Stability under Extension. Int. J. Damage Mechanics, 1955, 4, No 1, 58-82.

[2] G. A. Francfort and J.-J. Marigo, Stable damage evolution in a brittle continuous medium. European J. Mech. A Solids 12 (1993), no. 2, 149–189

[3] Timoshenko, S.P; Goodier, J. N. Theory of Elasticity. 2d ed. McGraw-Hill Book Company, Inc., New York, Toronto, London, 1951.

[4] L.I. Slepian, Models and Phenomena in Fracture Mechanics. Springer Verlag, 2002.

[5] Balk, A., Cherkaev, A. and Slepyan, L. Dynamics of Chains with Non-monotone Stress-strain Relations. I. Model and numerical experiments. J. Mech. Phys. Solids, 49, 2001, 131-148.

[6] Balk, A., Cherkaev, A. and Slepyan, L. Dynamics of Chains with Non-monotone Stress-strain Relations. II. Nonlinear Waves and Wave of Phase Transition. J. Mech. Phys. Solids, 49, 2001, 149-171.

[7] Slepyan, L. I.; Ayzenberg-Stepanenko, M. V. Some surprising phenomena in weak-bond fracture of a triangular lattice. J. Mech. Phys. Solids 50 (2002), no. 8, 1591–1625.

[8] Kyriafides, Stelios. Propagating Instabilities in Structures Advances in Applied Mechanics, v30, 68-186, 1994

[9] V. I. Nekorkin, M. G. Velarde. Synergetic Phenomena in Active Lattices. Springer Verlag, 2002.

[10] Morikazu Toda. Theory of nonlinear lattices. Springer Verlag, 1989.